

Paleoceanography and Paleoclimatology

RESEARCH ARTICLE

10.1029/2019PA003741

Key Points:

- At orbital scales, Chinese speleothem oxygen isotopes mainly represent the meridional migration of the East Asian monsoon circulation
- At orbital scales, low values of Chinese speleothem oxygen isotopes are associated with early northward movement of the East Asian rainbelt
- At interannual scales, Chinese speleothem oxygen isotope ratios are mainly controlled by the change of moisture source locations

Correspondence to:

J. Hu and J. Emile-Geay,
hujun@usc.edu; julieneg@usc.edu

Citation:

Hu, J., Emile-Geay, J., Tabor, C., Nusbaumer, J., & Partin, J. (2019). Deciphering oxygen isotope records from Chinese speleothems with an isotope-enabled climate model. *Paleoceanography and Paleoclimatology*, 34. <https://doi.org/10.1029/2019PA003741>

Received 31 JUL 2019

Accepted 27 NOV 2019

Deciphering Oxygen Isotope Records From Chinese Speleothems With an Isotope-Enabled Climate Model

Jun Hu¹, Julien Emile-Geay¹, Clay Tabor², Jesse Nusbaumer³, and Judson Partin⁴

¹Department of Earth Sciences, University of Southern California, Los Angeles, CA, USA, ²Department of Geosciences, University of Connecticut, Storrs, CT, USA, ³Climate and Global Dynamics Laboratory, National Center for Atmospheric Research, Boulder CO, USA, ⁴Institute for Geophysics, The University of Texas at Austin, Austin, TX, USA

Abstract Speleothem $\delta^{18}\text{O}$ is widely used to reconstruct past hydroclimate variability, particularly over Asia. However, the interpretation of this proxy is still in debate. While this proxy is originally interpreted as regional rainfall amount of the Asian monsoon, other studies have interpreted it as upstream monsoon rainfall or atmospheric circulation changes. To better understand the signal preserved in speleothems over various time scales, this study employs a state-of-the-art isotope-enabled climate model to quantify contributions to the oxygen isotope composition of precipitation ($\delta^{18}\text{O}_P$) over China. Results suggest that orbital-scale speleothem $\delta^{18}\text{O}$ variations at Chinese sites mainly record the meridional migration of the Asian monsoon circulation, accompanied by an early northward movement of the East Asian rain belt. At interannual scales, Chinese speleothem $\delta^{18}\text{O}$ is also tied to the intensity of monsoonal circulation, via a change in moisture source locations: Enhanced moisture delivery from remote source regions leads to more negative $\delta^{18}\text{O}_P$, particularly in late summer and early autumn. Our results have implications for the hydroclimatic interpretation of speleothem $\delta^{18}\text{O}$ from Chinese caves and suggest that this interpretation is time scale dependent.

1. Introduction

Speleothems are widely used to reconstruct past climate due to its high dating precision and temporal resolution (McDermott, 2004). Since the pioneering Hulu cave study of Wang et al. (2001), which for the first time revealed a well-dated speleothem record in the monsoon region and showed its coherent variability with Greenland ice-cores records, Chinese speleothems have been in the spotlight of the paleoclimate community (Cheng et al., 2009, 2012, 2016; Cosford et al., 2008; Dykoski et al., 2005; Hu et al., 2008; Yuan et al., 2004; Wang et al., 2008). Several Chinese speleothem $\delta^{18}\text{O}$ records are continuous, dating back to 600 kyr ago, coinciding well with Northern Hemisphere summer insolation intensity and dominated by precessional cycles (23 kyr) (Cheng et al., 2009, 2012, 2016; Wang et al., 2008; Zhang et al., 2019). The interpretation of these records remains in intense debates (Cheng et al., 2016; Liu et al., 2014). Chinese speleothem $\delta^{18}\text{O}$ records were originally interpreted as “monsoon intensity” because seasonal precipitation dominates the annual precipitation signal in these regions. Based on the local “amount effect” (i.e., the negative relationship between $\delta^{18}\text{O}_P$ and rainfall amount at the same site) (Dansgaard, 1964; Ishizaki et al., 2012; Lee & Fung, 2008; Risi et al., 2008), the precipitation $\delta^{18}\text{O}$ in the Asian monsoon region should represent the regional monsoon precipitation amount (Cheng et al., 2009, 2012; Hu et al., 2008; Yuan et al., 2004; Wang et al., 2001). This assumes that the local amount effect is dominant, yet other studies have shown other processes to be important: upstream rainout processes (Pausata et al., 2011), changes in moisture sources or atmospheric circulation pathways (Breitenbach et al., 2010; Liu et al., 2014; Maher & Thompson, 2012; Tabor et al., 2018; Tan, 2014), convective activity (Aggarwal et al., 2016; Kurita et al., 2011), karst system processes (Baker et al., 2013), and sea level changes (Xue et al., 2019). Thus, a more refined interpretation of oxygen isotope excursions in Chinese speleothems requires that all contributions be quantified.

Despite this complexity, many studies have noted that speleothem $\delta^{18}\text{O}$ at orbital scales is coherent across Asia, closely tracking Northern Hemisphere summer insolation (Battisti et al., 2014; Cheng et al., 2012, 2016). However, this coherency vanishes at scales shorter than millennial (Chu et al., 2012; Li et al., 2014; Wan et al., 2011; Zhang et al., 2019). This raises the question of what governs Asian speleothem

$\delta^{18}\text{O}$ over various spatial and temporal scales. A better interpretation of this quantity should lead to a better understanding and improved projections of hydroclimate variability in Asia, which affects the water supply of over 4 billion people.

A prerequisite to understanding the isotopic composition of speleothem calcite is understanding the isotopic composition of its primary input, precipitation $\delta^{18}\text{O}$ (henceforth, $\delta^{18}\text{O}_p$). Numerical simulations by water isotope-enabled climate models offer a valuable perspective in this regard, providing a physically grounded simulation of its relation to other climatic variables. Using such a tool, Pausata et al. (2011) simulated a Heinrich event and found that Chinese speleothem $\delta^{18}\text{O}$ is actually determined by the amount of precipitation over India, thus introducing the “upstream effect” and challenging the original monsoon rainfall amount or the “monsoon intensity” view. Later, Liu et al. (2014) conducted a time-slice simulation of the last 21,000 years and reconciled these two opinions, claiming that Chinese speleothem $\delta^{18}\text{O}$ does represent the “monsoon intensity,” with “intensity” mainly referring to southerly winds over China, working synergistically with upstream depletion to drive Chinese speleothem $\delta^{18}\text{O}$. On interannual time scales, Yang et al. (2016) emphasized the role of upstream depletion, monsoon intensity, and El Niño–Southern Oscillation by using a simulation of IsoGSM (Yoshimura et al., 2008). However, these simulations do not disentangle different processes, such as water vapor transport and local rainfall amount, which influence $\delta^{18}\text{O}_p$. A recent version of iCESM (Brady et al., 2019) is capable of tracking moisture and water isotopes by tagging water vapor evaporating from a specific region, which is key to quantifying the contributions of different factors to $\delta^{18}\text{O}_p$. This approach also has advantages over the back-trajectory method (Dirmeyer & Brubaker, 2007; Stein et al., 2015) since the latter requires high-frequency measurements of circulation and moisture fields to constrain errors and avoid artificial mixing (Singh et al., 2016; Stohl et al., 2004). Tabor et al. (2018) utilized this model and found that the change of remote moisture sources played a dominant role in the orbital variation of Indian speleothem $\delta^{18}\text{O}$. In this study, we will employ iCESM to investigate the interpretation of Chinese speleothem $\delta^{18}\text{O}$ at both orbital and interannual scales.

Another insight to understand the relationship between Chinese speleothem $\delta^{18}\text{O}$ and the Asian monsoon comes from modern monsoon studies. Chinese records reside in the East Asian monsoon region, which features monsoon dynamics distinct from its Indian and the West African counterparts: The East Asian monsoon is affected by both tropical and midlatitude systems, and it also features unique intraseasonal variability (Ding & Chan, 2005; Lau et al., 1988). Any description of the East Asian monsoon should include both rainfall and circulation systems: The prominent feature of the East Asian monsoon rainfall is the rainbelt from mid-June to mid-July, which is called mei-yu, extending from central eastern China to Japan (where the caves of Sanbao and Hulu are located, Figure 1); the circulation of the East Asian monsoon features westerly winds over the northern Indian Ocean and southerly winds over the South China Sea and Eastern China. Modern observations reveal a tripole pattern of the East Asian precipitation at interannual scales (Figure 1 in Zhang et al., 2018) (Day et al., 2015). In this mode, strong monsoon winds are associated with low precipitation in central China. Because of this decoupling of precipitation and circulation in the East Asian monsoon and the heterogeneity of the rainfall pattern, there are many definitions of the intensity of the East Asian summer monsoon. Among these definitions, some are based on regional rainfall amount while others are based on circulation metrics (Wang et al., 2008). Therefore, it is essential to clarify which aspects are grouped under the term “monsoon intensity,” and which ones—if any—dominate the interpretation of Chinese speleothem $\delta^{18}\text{O}$. Finally, the East Asian monsoon exhibits a unique subseasonal behavior, wherein the rainbelt abruptly “jumps” northward in summer along with the westerly jet, landing in northern China after July. If the rainbelt stays in central China longer, the rainy season there will be longer and yield more precipitation, which may affect $\delta^{18}\text{O}_p$. This unique seasonal change must be considered when interpreting Chinese speleothem $\delta^{18}\text{O}$ (Chiang et al., 2015; Kong et al., 2017; Yu & Zhou, 2007).

The paper is structured as follows: We first review the coherency of Asian speleothem records in Section 2 and introduce the model and numerical experiments in Section 3. Section 4 investigates the interpretations of $\delta^{18}\text{O}_p$ in China at orbital and interannual scales. Section 5 discusses the simulation biases and implications for other time scales, and Section 6 provides our conclusions.

2. Coherency Analysis of Chinese Speleothem $\delta^{18}\text{O}$ Records

In this section we review the coherency of Asian speleothems over orbital to decadal scales. The data used are from the National Centers for Environmental Information (<https://www.ncdc.noaa.gov/data-access/>

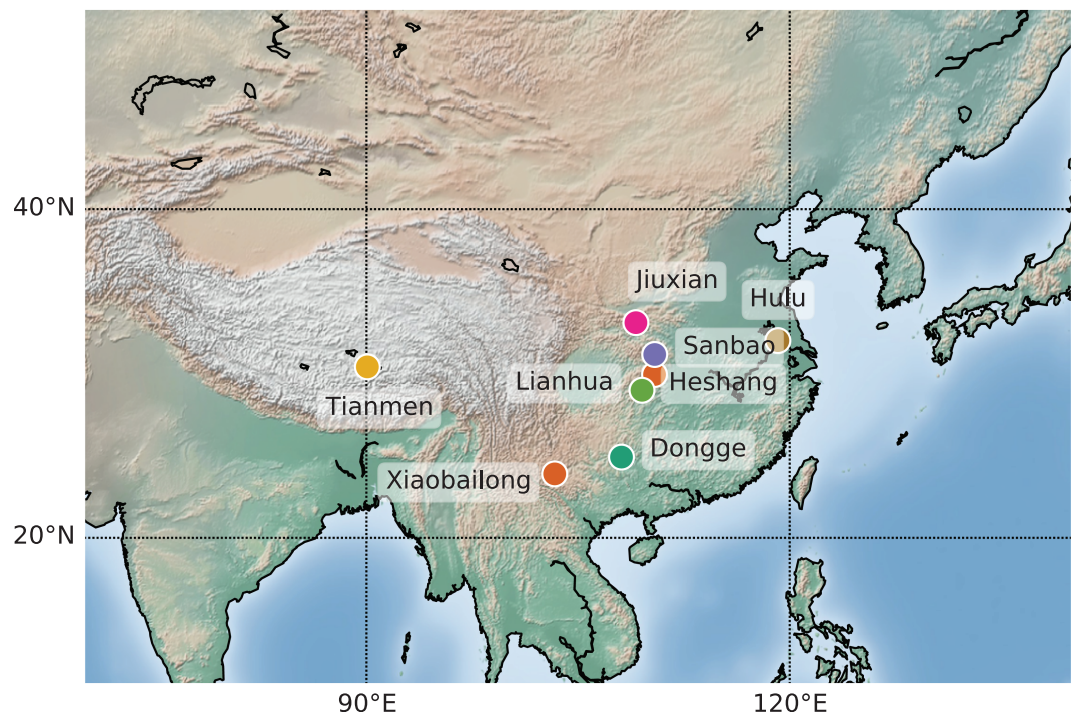


Figure 1. The spatial distribution of the Chinese speleothem records used in this section.

paleoclimatology-data/datasets/speleothem) with four speleothem records covering the last 400,000 years and seven records covering the last 11,000 years. Figure 1 shows the locations of these speleothem records.

Figure 2a shows the orbital variability of four speleothem $\delta^{18}\text{O}$ records in China. Their variability is coherent, and dominated by precession (Battisti et al., 2014; Cheng et al., 2016; Kathayat et al., 2016), and correlates well with local summer insolation. This coherency implies that Chinese speleothem $\delta^{18}\text{O}$ at orbital scales should represent a climate phenomenon at large spatial scales, and the prevailing inference is the regional rainfall amount (Cheng et al., 2016).

Recent studies have used speleothem $\delta^{18}\text{O}$ to study hydroclimate variability at suborbital time scales (Chen et al., 2016; Sinha et al., 2011, 2015; Tan et al., 2011, 2015; Yang et al., 2016) exploiting the high temporal resolution of speleothem data. Figure 2b shows Asian speleothem $\delta^{18}\text{O}$ over the Holocene. All records show a trend toward isotopic enrichment from 8,000 BP onward, following the trend of their local summer insolation. But if we zoom in on time scales shorter than millennial, the coherency vanishes (Figure 2c). This can be expected as the amplitude of speleothem $\delta^{18}\text{O}$ variations at these time scales about half what is observed at orbital scales (2–3‰ vs. 5–6‰), and other processes can interfere: regional climate variability, karst system processes (Baker & Bradley, 2010), and uncertainties in the age models (Hu et al., 2017).

We now leverage an isotope-enabled model to explain the interannual and orbital variability of speleothem $\delta^{18}\text{O}$ in China.

3. Experimental Design

We employ the water isotope-enabled version of the National Center for Atmospheric Research's Community Earth System Model Version 1 (iCESM1) (Brady et al., 2019). It is a state-of-the-art coupled climate model implementing water isotopes, composed of the atmospheric model iCAM5 (Nusbaumer et al., 2017), the ocean model iPOP2 (Zhang et al., 2017), the land model iCLM4 (Wong et al., 2017), the sea ice model iCICE4, the river transport model iRTM, and the CESM Coupler. The atmosphere model we use has a horizontal resolution of $1.875^\circ \times 2.5^\circ$ and 30 vertical levels. iCESM can simulate the variability of $\delta^{18}\text{O}_P$ and precipitation in the Asian monsoon region reasonably well (Brady et al., 2019; Nusbaumer et al., 2017; Tabor et al., 2018). It is the current best isotope-enabled model in simulating the relationship between $\delta^{18}\text{O}_P$ and

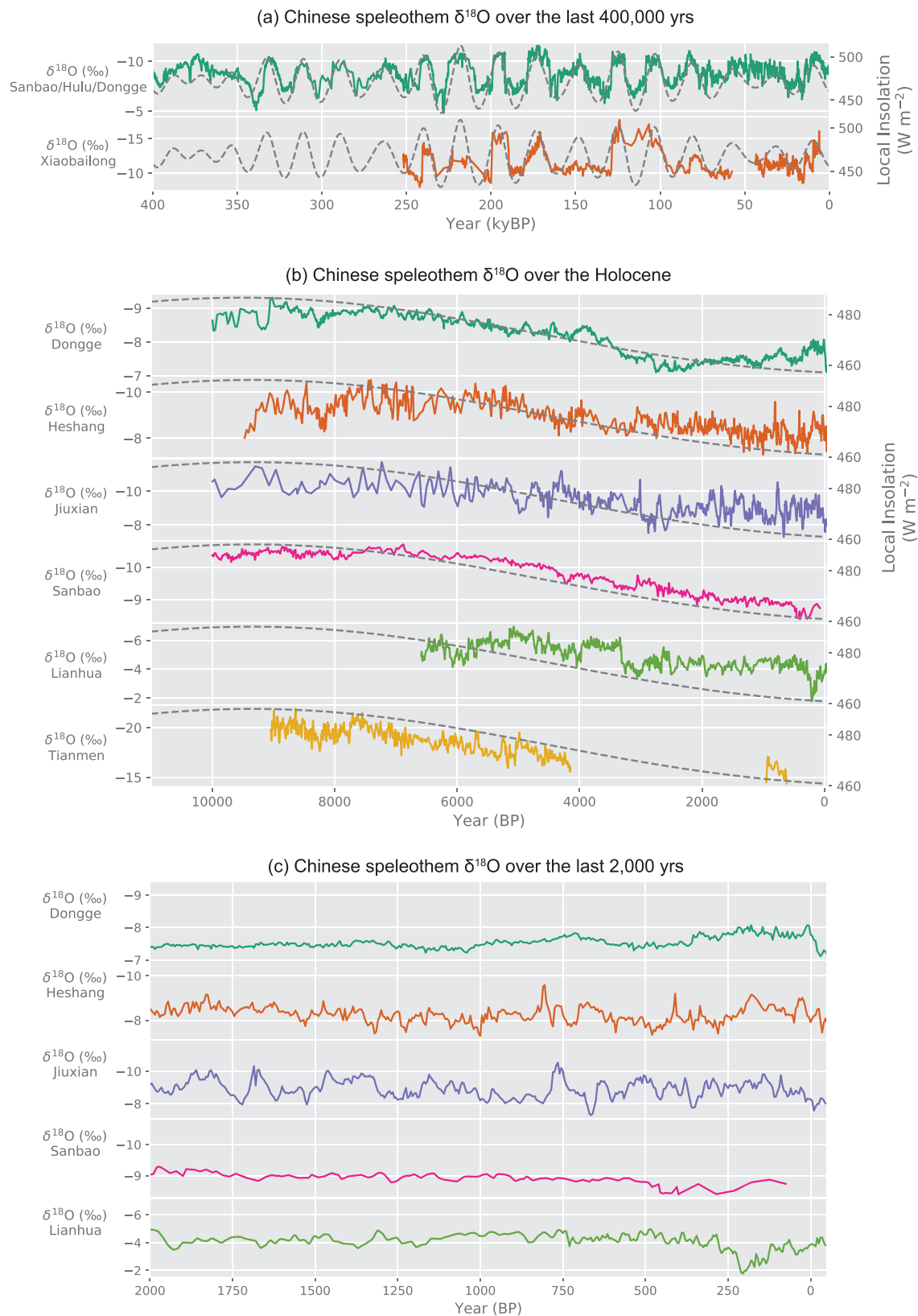


Figure 2. (a) Chinese speleothem $\delta^{18}\text{O}$ over the last 400,000 years (colored solid lines) with their local summer JJA insolation (gray dashed lines). $\delta^{18}\text{O}$ in the first panel is a composite of three Chinese records (Sanbao, Hulu, and Dongge Caves) in Cheng et al. (2016). (b) Chinese speleothem $\delta^{18}\text{O}$ over the Holocene with their local summer insolation. (c) Chinese speleothem $\delta^{18}\text{O}$ over the last 2,000 years.

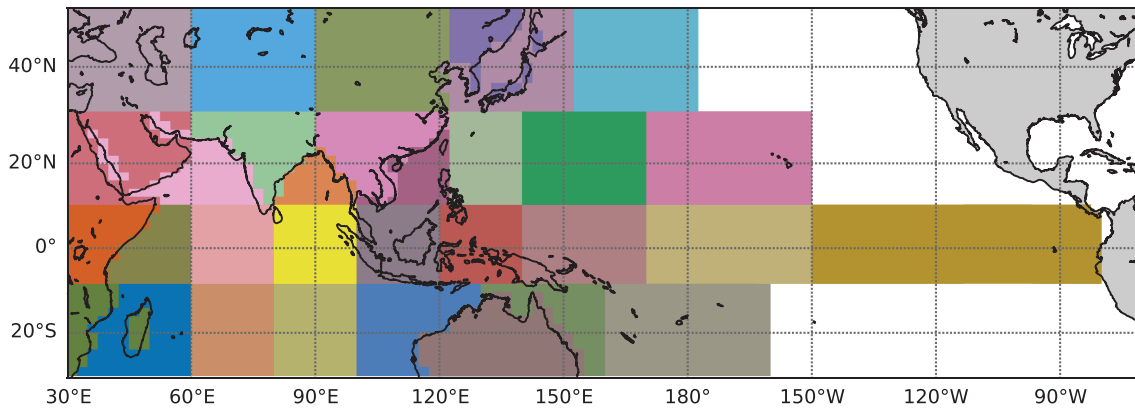


Figure 3. Tagged regions in the iCESM simulation from 1954–2012.

convective activity (Hu et al., 2018). Also, this version of iCESM has been modified to track moisture and water isotopes for specific regions by tagging water vapor once it evaporates from the surface. The tagged water vapor can be advected and goes through phase changes until it leaves the atmosphere as precipitation. There are already several studies using this water-tagging technique to track moisture and water isotopes (Dyer et al., 2017; Nusbaumer & Noone, 2018; Singh et al., 2016; Tabor et al., 2018).

For the study of the seasonal and interannual variability of speleothem $\delta^{18}\text{O}$, we conducted an experiment with prescribed sea surface temperature and sea ice observations from 1954–2012 and tag the water vapor originating from 32 regions shown in Figure 3. These regions are chosen because their total contribution of moisture contributes to 95% of precipitation in Asia.

$\delta^{18}\text{O}_P$ at one grid cell is the sum of $\delta^{18}\text{O}_P$ originating from all tagged regions, weighted by their precipitation contribution:

$$\delta^{18}\text{O}_P = \sum_{i=1}^{32} \delta^{18}\text{O}_{P_{\text{sink}_i}} \times \frac{P_i}{P_{\text{total}}} \quad (1)$$

where i indexes a tagged region, $\delta^{18}\text{O}_{P_{\text{sink}_i}}$ and P_i are $\delta^{18}\text{O}_P$ and precipitation falling at this grid cell (we call this cell “sink”) whose water vapor originates from the i th tagged region, respectively. P_{total} is the total precipitation at this grid cell. Tabor et al. (2018) developed a framework to decompose the change of $\delta^{18}\text{O}_P$ since $\delta^{18}\text{O}_{P_{\text{sink}_i}}$ can be seen as the sum of water vapor $\delta^{18}\text{O}$ at source location, change of water vapor $\delta^{18}\text{O}$ between the sink and source, and the difference between $\delta^{18}\text{O}_P$ and water vapor $\delta^{18}\text{O}$ at the sink:

$$(\delta^{18}\text{O}_P)_i = (\delta^{18}\text{O}_{P_{\text{sink}}} - \delta^{18}\text{O}_{\text{wv}_{\text{sink}}})_i + (\delta^{18}\text{O}_{\text{wv}_{\text{sink}}} - \delta^{18}\text{O}_{\text{wv}_{\text{source}}})_i + (\delta^{18}\text{O}_{\text{wv}_{\text{source}}})_i \quad (2)$$

Thus the change of precipitation between two climate states can be decomposed into four terms:

$$\begin{aligned} \Delta(\delta^{18}\text{O}_P)_i &= \Delta \left(\delta^{18}\text{O}_{P_{\text{sink}_i}} \times \frac{P_i}{P_{\text{total}}} \right) \\ &= \Delta \left[\underbrace{(\delta^{18}\text{O}_{P_{\text{sink}}} - \delta^{18}\text{O}_{\text{wv}_{\text{sink}}})_i}_{\text{Condensation}} + \underbrace{(\delta^{18}\text{O}_{\text{wv}_{\text{sink}}} - \delta^{18}\text{O}_{\text{wv}_{\text{source}}})_i}_{\text{Rainout}} + \underbrace{(\delta^{18}\text{O}_{\text{wv}_{\text{source}}})_i}_{\text{Source composition}} \right] \times \left(\frac{P_i}{P_{\text{total}}} \right) \\ &\quad + \underbrace{\delta^{18}\text{O}_{P_{\text{sink}_i}} \times \Delta \left(\frac{P_i}{P_{\text{total}}} \right)}_{\text{Source location changes.}} \end{aligned} \quad (3)$$

The first three terms are related to the change of $\delta^{18}\text{O}_P$ at the sink. This first term is about the change due to phase changes at the sink, which is about the change of condensation, so we call this term “condensation

changes.” This term includes the condensation of water vapor and reevaporation of raindrops in convective and large-scale precipitation processes occurring at subgrid scales, so it partially reflects the impact of convection on $\delta^{18}\text{O}_P$. The second term is about the change of the difference between moisture source and sink, and this is generally due to the change in travel distance and/or upstream rainout, so we call this term “rainout changes.” The third term tracks changes due to water vapor $\delta^{18}\text{O}$ at the moisture source, so we call this term “source composition changes.” The last term arises because of the change of precipitation contribution from each tagged region, which describes the change of moisture source location, so we will call this term “source location change.” It should be noted that the parts without changes (i.e., without the notation of Δ , including $\delta^{18}\text{O}_{P_{\text{sink}_i}}$ and $\frac{P_i}{P_{\text{total}}}$) are calculated with the climate mean values (i.e., the averaged values of the entire simulation); therefore, moisture source location changes also include the influence of the climate mean of $\delta^{18}\text{O}_{P_{\text{sink}_i}}$. For clarity, in the paper, local “amount effect” refers to the negative relationship between $\delta^{18}\text{O}_P$ and rainfall amount at the same site. The view of “monsoon intensity” refers to the interpretation of speleothem $\delta^{18}\text{O}$ as regional monsoon rainfall amount.

For orbital variability, we analyzed the orbital forcing experiments of Tabor et al. (2018). There are four simulations with different precession angles with the maximum eccentricity value of the past 900 kyr (0.0493). The four angles are Northern Hemisphere perihelion at autumnal equinox, winter solstice, vernal equinox, and summer solstice. The simulations were branched from equilibrium simulations and run for 550 years, and the analyses come from the average of the last 48 years.

4. Results

4.1. Orbital Variability

We analyzed the experiments in the same configurations of precession minimum (Northern Hemisphere perihelion at summer solstice, henceforth, P_{\min} , when the Northern Hemisphere summer insolation reaches a maximum) and precession maximum (Northern Hemisphere perihelion at winter solstice, henceforth, P_{\max} , when the Northern Hemisphere summer insolation reaches a minimum) as Tabor et al. (2018). Here we mainly focus on the monsoon season (May–September, MJJAS) of East China, which contributes the majority of the annual precipitation there. There is a significant contrast of precipitation (>5 mm/day) between the onset of the monsoon season and winter (Wang, 2002). Figure 4a shows the difference of climatological weighted $\delta^{18}\text{O}_P$ between P_{\min} and P_{\max} . Since there is a recharge threshold for rainfall infiltrating through karst systems, only months with precipitation amount larger than 150 mm/month are used to calculate the weighted $\delta^{18}\text{O}_P$ (Baker et al., 2019; Jones & Banner, 2003; Partin et al., 2012). It indicates that iCESM can simulate more negative weighted $\delta^{18}\text{O}_P$ in P_{\min} in the central and southern China as we expect based on speleothem records, but the amplitude is weaker (-1.6% , compared with ~ -4 to 5% in speleothem $\delta^{18}\text{O}$). The negative anomaly only extends to 30°N , and we will discuss the possible reasons for this bias in Section 5.

The difference in circulation and $\delta^{18}\text{O}_P$ anomaly of the monsoon season (MJJAS) between the P_{\min} and P_{\max} is shown in Figure 4b. It generally displays a strengthening of the northern part of the Asian summer monsoon low-level circulation, which indicates a northward movement of both the Indian and East Asian summer monsoon. It is also noticeable that the subtropical high over the North Pacific also moves northward. Thus, both the subtropical and monsoon systems move northward when the Northern Hemisphere receives more summer insolation. The convergence maxima of low-level (850 hPa) winds around the equatorial Indian Ocean can be used to measure the migration of monsoon winds. Here we take the mean latitude of zero speed of zonal wind over the tropical Indian Ocean (10°S to 10°N , 35 – 60°E) to quantify that. In our simulation, the Asian monsoon moves 4° northward. At 850 hPa, all monsoon-related circulation, including Somali jet, the eastward winds over the northern Indian Ocean, and southerly winds over the South China Sea, moves northward. However, this northward migration does not translate into a uniform increase in precipitation. Figure 4c shows that MJJAS precipitation in central China and Japan is less in P_{\min} , while precipitation in northern and southern China, India, and West Asia is larger. This pattern is similar to the leading mode of interannual precipitation variability in East Asia (Day et al., 2015). Speleothem trace element ratios also suggest that low values of speleothem $\delta^{18}\text{O}$ in central China can coincide with dryness instead of wetness in that region (Zhang et al., 2018). This, however, is not enough to reach a conclusion regarding central China receiving less precipitation in P_{\min} , since similar simulations with other models like EC-Earth and GFDL-CM2.1 do not clearly show less precipitation in central China (Bosmans

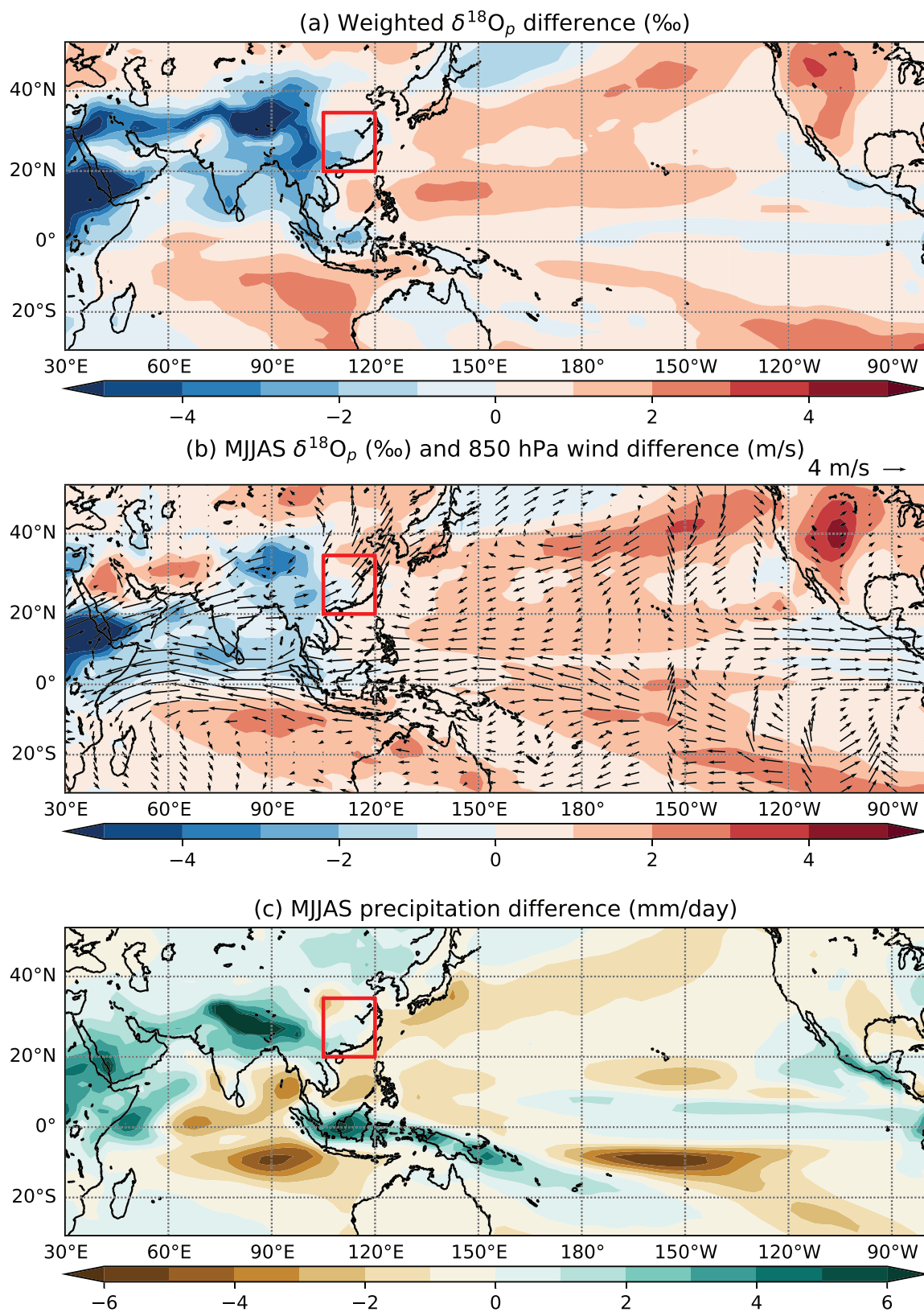


Figure 4. Difference between precession minimum (maximum of the Northern Hemisphere summer insolation) and maximum (minimum of the Northern Hemisphere summer insolation). (a) Weighted $\delta^{18}\text{O}_p$ difference, (b) MJJAS $\delta^{18}\text{O}_p$ and 850-hPa wind difference. (c) MJJAS precipitation difference. The red box is the defined region of East China, and its mean precipitation and $\delta^{18}\text{O}_p$ is in Figures 5a and 5b.

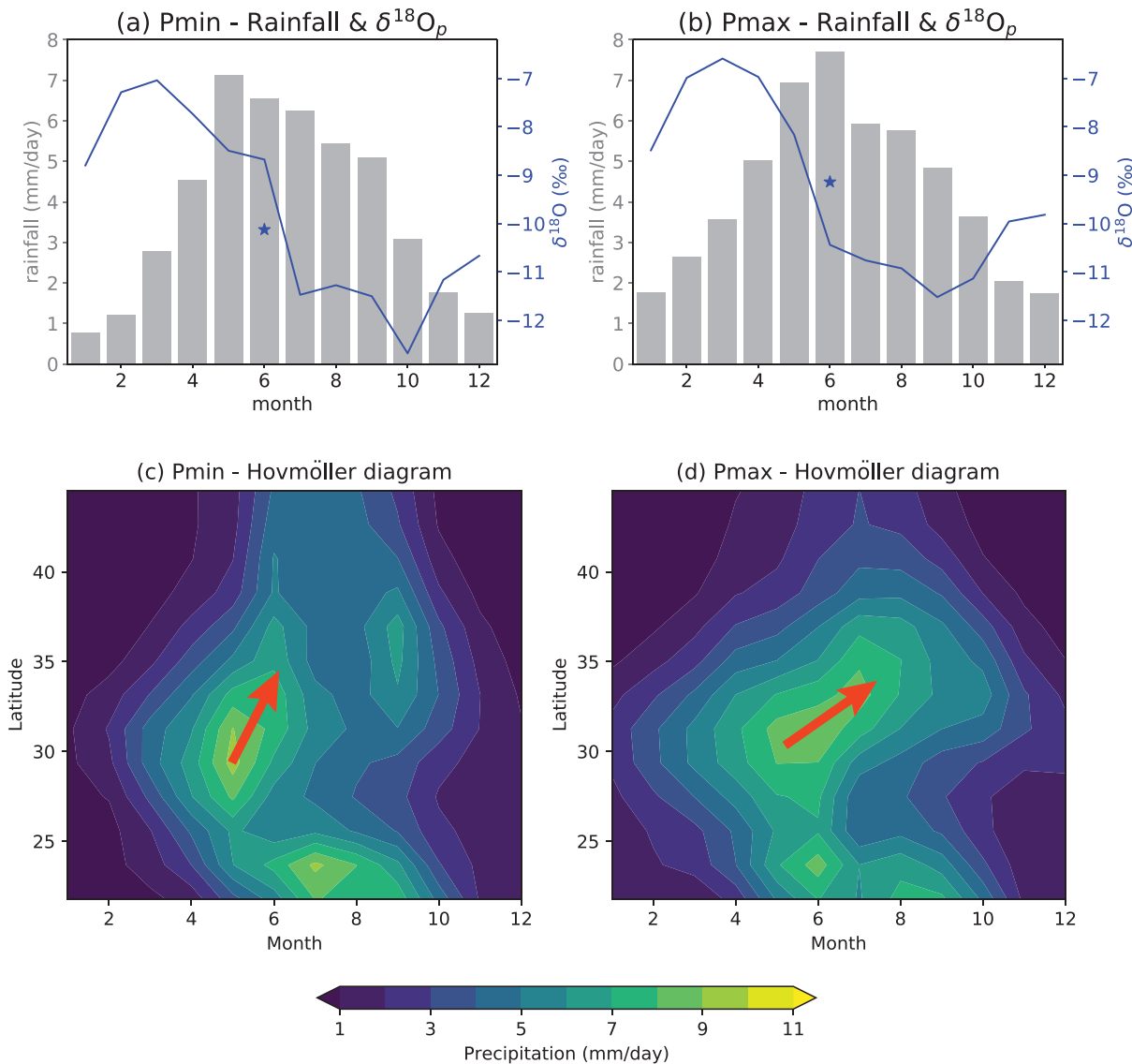


Figure 5. Climatological monthly mean precipitation in East China ($20\text{--}35^\circ\text{N}$, $105\text{--}120^\circ\text{E}$) in precession minimum (a) and precession maximum (b). The star signs show the values of weighted $\delta^{18}\text{O}_p$. Hovmöller diagram of climatological monthly mean precipitation in East China in precession minimum (c) and precession maximum (d).

et al., 2018). These models all show a northward migration of the East Asian monsoon circulation. In short, the $\delta^{18}\text{O}_p$ change in China at orbital scales represents the northward extension of the East Asian monsoon circulation, not the monsoon precipitation. If one must use the term “monsoon intensity” to interpret China $\delta^{18}\text{O}$ records, this term should refer to the northward migration of the large-scale monsoon circulation rather than enhanced local monsoon rainfall. This is consistent with the conclusion of Liu et al. (2014), which states that the $\delta^{18}\text{O}$ records represent enhanced southerly monsoon winds over south China, though we also point out the northward migration of the monsoon winds together with its strengthening. It should be noted that circulation shifts alone would not produce changes in $\delta^{18}\text{O}_p$. The circulation shifts generate changes in moisture source locations or rainout processes, which directly affect $\delta^{18}\text{O}_p$, and we will discuss the details later.

The northward extension of the monsoon circulation is accompanied by a change in seasonality. The annual cycle of precipitation in East China (Figures 5a and 5b) shows that in P_{\min} the precipitation maximum occurs in May rather than June. The Hovmöller diagram of East Asian precipitation (Figures 5c and 5d) shows that in P_{\min} the rainbelt builds in May around 30°N , and then moves northward quickly to 40°N in June,

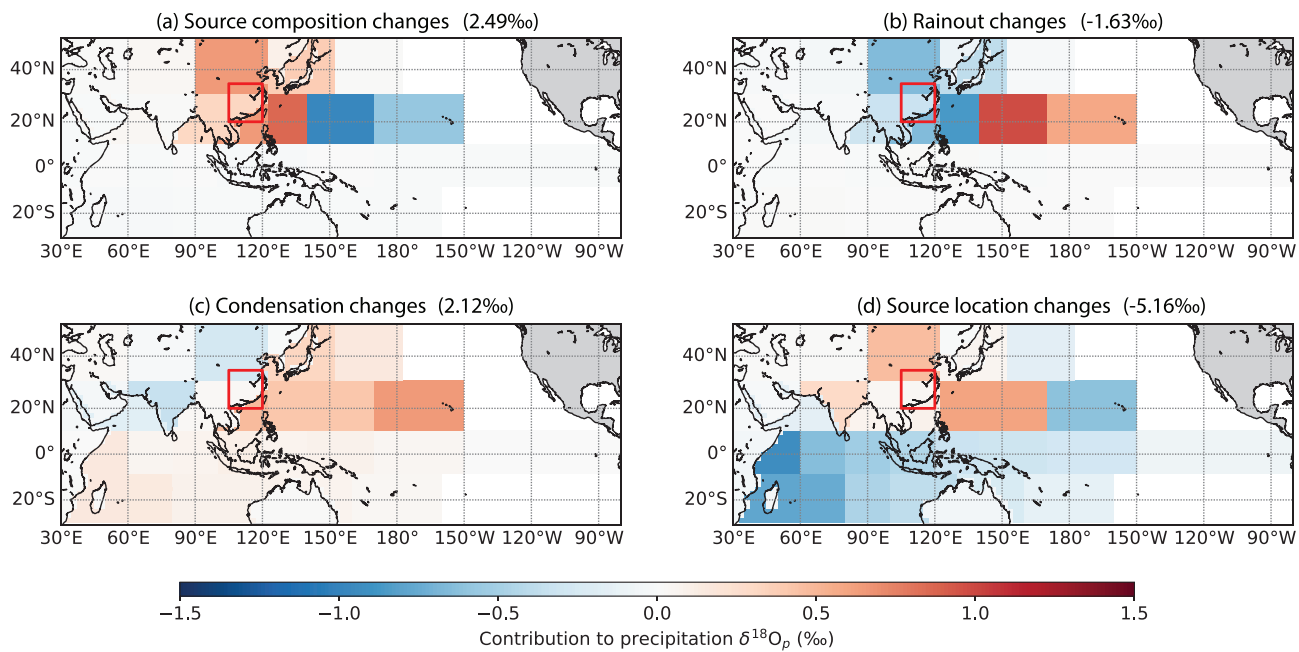


Figure 6. Decomposition of seasonal differences in $\delta^{18}\text{O}_p$ as an analog for precessional variations. The figure shows the contribution of (a) moisture source composition, (b) rainout changes, (c) condensation changes, and (d) moisture location changes to $\delta^{18}\text{O}_p$ over East China from tagged regions. The $\delta^{18}\text{O}$ values in the subtitles of each subplot are the summed contribution of these four factors.

while in P_{\max} the rainbelt moves northward slower, reaching 35°N in August. These results point out that in P_{\min} , the rainy season in central China, mei-yu, home to many famous cave sites, comes one month earlier and its duration is shortened, which leads to less precipitation there. This is consistent with the simulation results by Kong et al. (2017), which shows an earlier onset and a shortening of mei-yu in the early Holocene when the Northern Hemisphere received more insolation in summer, compared to the late Holocene. Kong et al. (2017) propose that the insolation increase in summer reduces the pole-equator temperature gradient, which leads to the earlier northward shift of westerlies, causing the early onset and shortening of mei-yu in central China.

Seasonal differences in $\delta^{18}\text{O}_p$ may be used as an analog for precessional variations, since the impacts of precessional forcing can be viewed as amplified summer-winter contrasts. Thus, we analyze the difference between boreal summer and winter in our AMIP-like water-tagging experiment. With the decomposition framework, we separate the contributions from moisture source composition, rainout processes, condensation processes, and moisture source location. Figure 6 shows that the change of moisture source location contributes most to the more negative $\delta^{18}\text{O}_p$ of East China in summer. It contributes -5.06‰ to the total seasonal difference of -2.08‰ if we sum up the contributions of each tagging regions. (See the numbers in each subplot of Figure 6.) The source location factor contributes to more negative $\delta^{18}\text{O}$ because more moisture comes from the Indian Ocean, which makes $\delta^{18}\text{O}_p$ in China more negative (Figure 6d). The change of rainout also contributes to more negative $\delta^{18}\text{O}$ (-1.63‰) in summer. We should note from Figure 6 that the contributions from different tagging regions can offset each other. Taking rainout changes, for instance, regions near East Asia contribute negative $\delta^{18}\text{O}$, but remote Pacific regions contribute positive $\delta^{18}\text{O}$, and the sum of all contributions is negative. If this also applies to orbital variability, this result implies that speleothem $\delta^{18}\text{O}$ in China is controlled by both rainout changes and moisture source location changes. For central China, since the model result suggests less precipitation in P_{\min} , changes in the moisture source location may play a more significant role—more moisture comes from the Indian Ocean and less moisture comes from the Northwestern Pacific. These changes of moisture source location are the result of the meridional migration of the large-scale monsoon circulation discussed above.

4.2. Interannual Variability

In addition to orbital-scale variability, the interannual-decadal variability of Chinese speleothem records is also of great interest (Chen et al., 2016; Tan et al., 2011; 2015; Yang et al., 2016). This variability has been

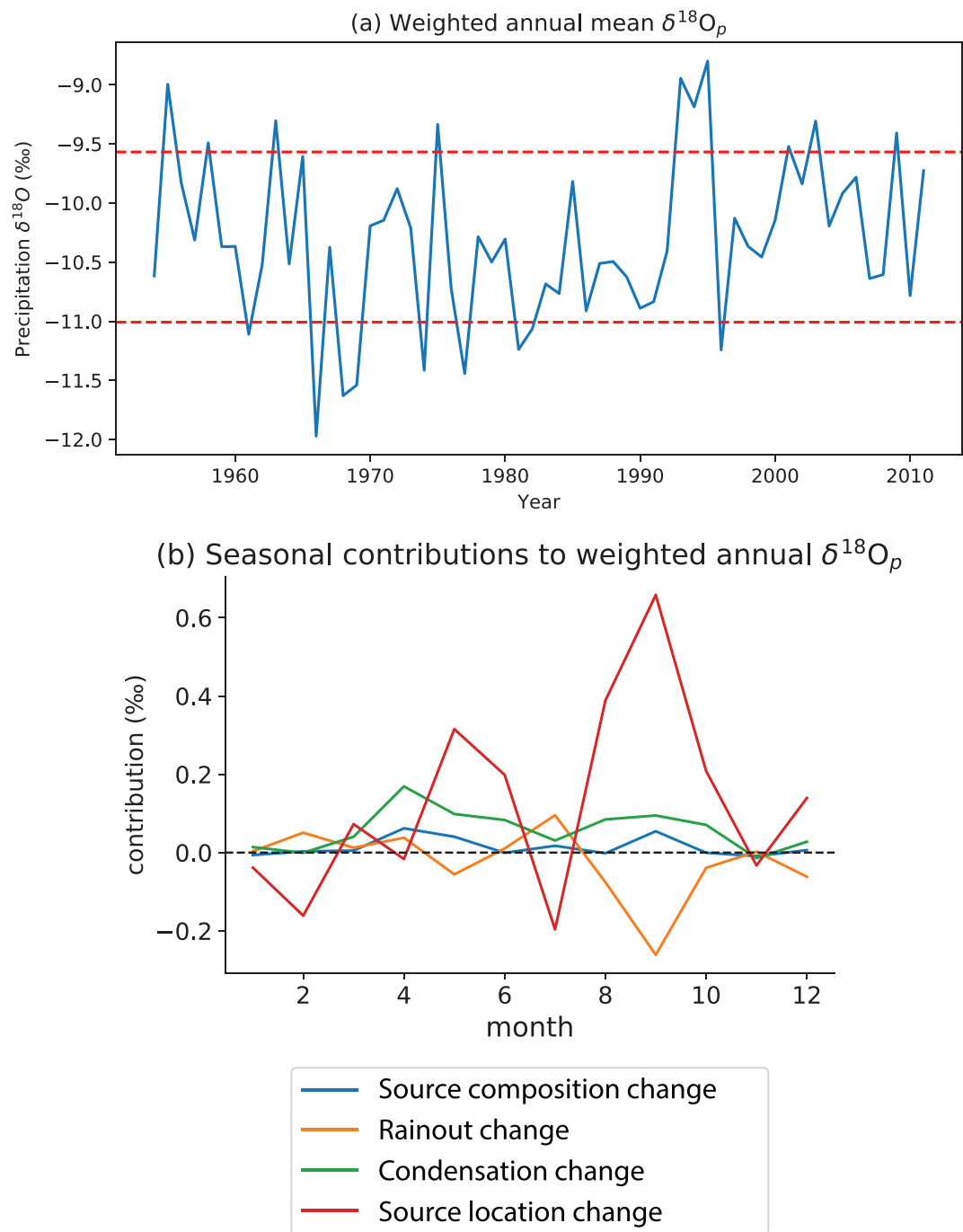


Figure 7. (a) Time series of weighted annual mean $\delta^{18}\text{O}_p$ in East China from the 59-year-long model simulation (1954–2012). The red dashed lines are one standard deviation above and below the mean. (b) Seasonal contributions of four factors to weighted annual $\delta^{18}\text{O}_p$ in East China based on the model simulation.

interpreted as monsoon intensity, changes in El Niño–Southern Oscillation intensity, and moisture source location changes.

Here we discuss what factors control the interannual variability of $\delta^{18}\text{O}_p$ in East China based on the AMIP-like water-tagging experiment. We spatially average the precipitation weighted annual $\delta^{18}\text{O}_p$ in East China (red box in Fig 8) to generate a time series of East China $\delta^{18}\text{O}_p$ (Figure 7a). We then select high $\delta^{18}\text{O}$ years if their values are above one standard deviation from the mean value and select low $\delta^{18}\text{O}$ years if their values are below one standard deviation from the mean. We make composites of high $\delta^{18}\text{O}$ years

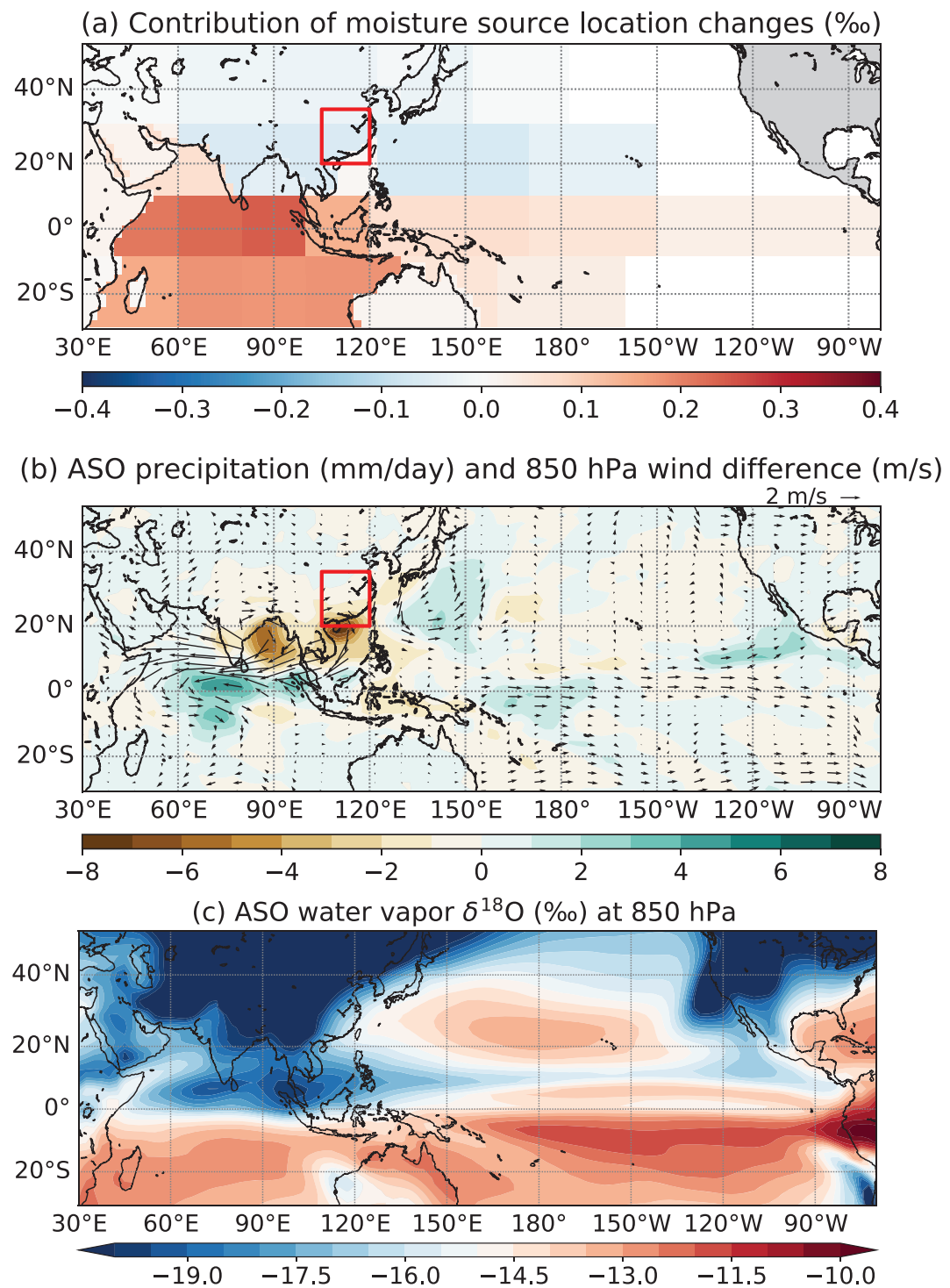


Figure 8. (a) Contribution of moisture source location changes to the interannual variability of East China $\delta^{18}\text{O}_P$ from tagged regions. (b) Difference of 850-hPa wind and precipitation in ASO between high and low $\delta^{18}\text{O}_P$ years of East China. (c) Climatological water vapor $\delta^{18}\text{O}$ at 850 hPa in ASO. The red rectangular is the defined East China region ($20\text{--}35^\circ\text{N}$, $105\text{--}120^\circ\text{E}$).

($n = 10$) and low $\delta^{18}\text{O}$ years ($n = 8$). The difference of the composites are decomposed into four factors by the previous framework. If we sum up the contribution from different tagging regions, we obtain the contributions shown in Figure 7b.

The result shows that, on interannual scales, $\delta^{18}\text{O}_P$ in East China is dominated by moisture source location changes, and its main contribution is in August to October. This suggests that the late monsoon season is likely to contribute more than other months to the monthly weighted $\delta^{18}\text{O}$ signal and, therefore, the speleothem $\delta^{18}\text{O}$ signal. When unfolding the contributions from the moisture source location changes, we can see that the Indian Ocean contributes most to the positive (negative) $\delta^{18}\text{O}$ anomalies in high (low) $\delta^{18}\text{O}$ years (Figure 8a). This is because more (less) moisture comes from the nearby land and ocean regions such as the northwestern Pacific and the Bay of Bengal, but less (more) moisture comes from the remote Indian Ocean. The water vapor $\delta^{18}\text{O}$ originating from remote places is generally more negative than from nearby regions due to an increase in rainout caused by the air mass having to travel farther from source to sink and thus experiencing more precipitation events. Also, water vapor over the northern Indian Ocean is more negative than that over the northwestern Pacific because of intense rainfall over the Indian Ocean and Maritime Continent (Figure 8c). This result is similar to that of Tabor et al. (2018) on the orbital variability of the Indian Monsoon in that the moisture source changes mainly control $\delta^{18}\text{O}_P$ variability. It should be noted that $\delta^{18}\text{O}_{P_{\text{sink}}}$, which is precipitation $\delta^{18}\text{O}$ falling at the study site whose water vapor originates from the i th tagged region, is in the term of moisture source changes. (Please refer to equation 3.) Thus, the rainout effect of the climatological mean is also embedded in this term, though the change in the rainout effect is not.

The difference of atmospheric circulation and precipitation between high and low $\delta^{18}\text{O}_P$ years is shown in Figure 8b. The low-level circulation anomaly in high $\delta^{18}\text{O}$ years is akin to a weakening of the monsoon circulation across South and East Asia, therefore bringing less moisture from the Indian Ocean. We can see that there are anticyclonic anomalies in the Bay of Bengal and East China Sea. These anomalies lead to more moisture coming from the Bay of Bengal and the northwestern Pacific. There is indeed less precipitation in East China in high $\delta^{18}\text{O}$ years, but the amplitude is too small to explain the positive $\delta^{18}\text{O}_P$ anomalies.

In summary, based on our model simulations, the interannual variability of $\delta^{18}\text{O}_P$ in East China is mainly controlled by moisture source changes—in years of high $\delta^{18}\text{O}_P$, less moisture comes from the Indian Ocean and more moisture from the northwestern Pacific, and high $\delta^{18}\text{O}_P$ represents a weakening of the Asian monsoon circulation. Conversely, low $\delta^{18}\text{O}_P$ represents enhanced Asian monsoon circulation. This provides a new interpretation of interannual variability of $\delta^{18}\text{O}_P$ and its related paleoclimate records in East China.

5. Discussion

We argue that the variation of Chinese speleothem $\delta^{18}\text{O}$ at orbital scales is largely controlled by both moisture source location changes and rainout changes, which vary as a function of the meridional migration of the large-scale monsoon circulation. The mean latitude of the convergence maxima of low-level monsoon winds over the tropical Indian Ocean (10°S to 10°N , $35\text{--}60^{\circ}\text{E}$) moves 4° northward in the precession minimum simulation compared to the modern climatology. Also, the water-tagging experiment result suggests that the change of Chinese speleothem $\delta^{18}\text{O}$ at orbital scales is largely due to the change of moisture source location.

We notice that at orbital scales, iCESM simulates a relatively weak $\delta^{18}\text{O}_P$ response to precessional forcing in East China. Based on Figure 6, the moisture source location change dominates the variation of Chinese $\delta^{18}\text{O}_P$ at orbital scales, assuming that other aspects of the model are correct, so the bias of $\delta^{18}\text{O}_P$ can be partly explained by the discrepancy of the model in simulating the moisture source location change responding to precessional forcing. Figure 4 shows that the north Pacific subtropical high strengthens together with the Asian monsoon circulation, and more moisture from the north Pacific subtropical high makes Chinese $\delta^{18}\text{O}_P$ more positive since it is closer than the Indian Ocean. It is possible that the subtropical high response is more intense than it should be in P_{min} , so its positive $\delta^{18}\text{O}_P$ contribution dampens the $\delta^{18}\text{O}_P$ response to precession forcing in East China. This weak response of $\delta^{18}\text{O}_P$ in East Asia seems common in isotope-enabled climate models such as ECHAM4.6 (Battisti et al., 2014; Roe et al., 2016) and iLOVECLIM (Caley et al., 2014) and needs further investigation. In addition, in our decomposition framework, we mainly quantify the contribution of source water vapor $\delta^{18}\text{O}$, rainout, and changes of moisture source distribution. The impact of local convection is included in the “condensation changes” term, but this term also includes large-scale

condensation, so future work is necessary to disentangle the effects of convection alone. Also, the convective activity occurring along water vapor pathways affect the “rainout” term. To quantify the contribution of convection to $\delta^{18}\text{O}_P$, we can employ a similar tagging technique to tag condensation and evaporation processes in convection schemes in the future. Furthermore, karst system processes can distort $\delta^{18}\text{O}_P$ signals, and shelf exposure is likely to affect speleothem $\delta^{18}\text{O}$ records near coastal regions. These processes are not included in the model employed in this study. Further investigations are needed to quantify their contributions to speleothem $\delta^{18}\text{O}$.

While our results are based on the numerical experiments, comparing speleothem $\delta^{18}\text{O}$ with other proxy data can provide additional clues to interpret speleothem $\delta^{18}\text{O}$. For example, Zhang et al. (2018) compared a speleothem $\delta^{18}\text{O}$ record with a speleothem trace metal record, which is believed to represent local precipitation and revealed the decoupling of precipitation and speleothem $\delta^{18}\text{O}$ signals. Also, a recent finding of marine sediments in the East China Sea (Clemens et al., 2018, Site U1429 of the International Ocean Discovery Program) representing the monsoon runoff showed that it did not feature the 23-kyr cycles present in speleothem records. Although this discrepancy can be explained by the possibility that the $\delta^{18}\text{O}$ signal in this marine sediment is also influenced by shoreline migration due to sea level changes, and speleothem $\delta^{18}\text{O}$ represents large-scale circulation variations as stated in this paper rather than local rainfall amount, this finding still should make us rethink why speleothem $\delta^{18}\text{O}$ primarily responds to insolation in the precessional band.

We mainly discussed the interpretation of Asian speleothem $\delta^{18}\text{O}$ at orbital and interannual time scales but did not cover the time scales in between. Asian speleothem $\delta^{18}\text{O}$ are coherent at millennial scales and follow the Northern Hemisphere insolation variations (Cheng et al., 2012, 2016; Zhang et al., 2019), so we believe its explanations will be similar with that at orbital scales, which is the migration of the monsoon circulation system. However, the change of regional precipitation patterns may not be the same as the orbital variations. For example, Pausata et al. (2011) simulated climate during the Heinrich events and found no obvious precipitation changes in China, while our study and other simulations (Bosmans et al., 2018) for orbital forcing show substantial precipitation changes in China. There are already studies showing the coherency of Asian speleothem $\delta^{18}\text{O}$ vanishes at scales shorter than millennial (Chu et al., 2012; Li et al., 2014; Wan et al., 2011; Zhang et al., 2019), and further investigations are needed to identify at which time scales the coherency disappears. Whether the external forcing or the internal variability of the atmosphere-land-ocean system dominates also needs further investigations by coupled climate models. For the interpretation of interannual variability of speleothem $\delta^{18}\text{O}$, we mainly focus on $\delta^{18}\text{O}_P$, and future work needs to be done to investigate to what extent the karst system processes and age uncertainty influence the heterogeneity of Asian speleothem records.

6. Conclusion

We investigated the interpretation of Chinese speleothem $\delta^{18}\text{O}$ via the isotope-enabled model iCESM. The results show that Chinese speleothem $\delta^{18}\text{O}$ variations at orbital scales mainly represent the meridional migration of the East Asian monsoon circulation. These circulation changes lead to moisture source location and rainout changes, which cause the $\delta^{18}\text{O}_P$ variations in China. This is also accompanied by the early northward movement of the East Asian rainbelt. The interannual variability of Chinese speleothem $\delta^{18}\text{O}$ is mainly controlled by the change of moisture source locations. More moisture coming from remote regions leads to more negative speleothem $\delta^{18}\text{O}$, and its influence is greatest in late summer and early autumn.

Acknowledgments

This work was supported by a Dornsife Merit Fellowship from the University of Southern California (USC). The authors would like to thank two anonymous reviewers, Dr. Lachnit and Dr. Jess Adkins, for their constructive suggestions. The experiment data used in the study are available online (<http://doi.org/10.5281/zenodo.3354638>).

References

- Aggarwal, P. K., Romatschke, U., Araguas-Araguas, L., Belachew, D., Longstaffe, F. J., Berg, P., et al. (2016). Proportions of convective and stratiform precipitation revealed in water isotope ratios. *Nature Geoscience*, 9(8), 624.
- Baker, A., & Bradley, C. (2010). Modern stalagmite $\delta^{18}\text{O}$: Instrumental calibration and forward modelling. *Global and Planetary Change*, 71(3), 201–206.
- Baker, A., Bradley, C., & Phipps, S. J. (2013). Hydrological modeling of stalagmite $\delta^{18}\text{O}$ response to glacial-interglacial transitions. *Geophysical Research Letters*, 40, 3207–3212. <https://doi.org/10.1002/grl.50555>
- Baker, A., Hartmann, A., Duan, W., Hankin, S., Comas-Bru, L., Cuthbert, M. O., et al. (2019). Global analysis reveals climatic controls on the oxygen isotope composition of cave drip water. *Nature Communications*, 10(1), 2984.
- Battisti, D., Ding, Q., & Roe, G. (2014). Coherent pan-Asian climatic and isotopic response to orbital forcing of tropical insolation. *Journal of Geophysical Research: Atmospheres*, 119, 11–997. <https://doi.org/10.1002/2014JD021960>

- Bosmans, J., Erb, M., Dolan, A., Drijfhout, S., Tuenter, E., Hilgen, F., et al. (2018). Response of the Asian summer monsoons to idealized precession and obliquity forcing in a set of GCMS. *Quaternary Science Reviews*, 188, 121–135.
- Brady, E., Stevenson, S., Bailey, D., Liu, Z., Noone, D., Nusbaumer, J., et al. (2019). The connected isotopic water cycle in the Community Earth System Model version 1. *Journal of Advances in Modeling Earth Systems*, 11, 2547–2566. <https://doi.org/10.1029/2019MS001663>
- Breitenbach, S. F., Adkins, J. F., Meyer, H., Marwan, N., Kumar, K. K., & Haug, G. H. (2010). Strong influence of water vapor source dynamics on stable isotopes in precipitation observed in Southern Meghalaya, NE India. *Earth and Planetary Science Letters*, 292(1), 212–220.
- Caley, T., Roche, D. M., & Renssen, H. (2014). Orbital Asian summer monsoon dynamics revealed using an isotope-enabled global climate model. *Nature Communications*, 5, 5371.
- Chen, S., Hoffmann, S. S., Lund, D. C., Cobb, K. M., Emile-Geay, J., & Adkins, J. F. (2016). A high-resolution speleothem record of western equatorial Pacific rainfall: Implications for Holocene ENSO evolution. *Earth and Planetary Science Letters*, 442, 61–71.
- Cheng, H., Edwards, R. L., Broecker, W. S., Denton, G. H., Kong, X., Wang, Y., et al. (2009). Ice age terminations. *Science*, 326(5950), 248–252.
- Cheng, H., Edwards, R. L., Sinha, A., Spötl, C., Yi, L., Chen, S., et al. (2016). The Asian monsoon over the past 640,000 years and ice age terminations. *Nature*, 534(7609), 640–646.
- Cheng, H., Sinha, A., Wang, X., Cruz, F. W., & Edwards, R. L. (2012). The global paleomonsoon as seen through speleothem records from Asia and the Americas. *Climate Dynamics*, 39(5), 1045–1062.
- Chiang, J. C., Fung, I. Y., Wu, C.-H., Cai, Y., Edman, J. P., Liu, Y., et al. (2015). Role of seasonal transitions and westerly jets in East Asian paleoclimate. *Quaternary Science Reviews*, 108, 111–129.
- Chu, P. C., Li, H.-C., Fan, C., & Chen, Y.-H. (2012). Speleothem evidence for temporal-spatial variation in the East Asian Summer Monsoon since the Medieval Warm Period. *Journal of Quaternary Science*, 27(9), 901–910.
- Clemens, S., Holbourn, A., Kubota, Y., Lee, K., Liu, Z., Chen, G., et al. (2018). Precession-band variance missing from East Asian monsoon runoff. *Nature Communications*, 9(1), 3364.
- Cosford, J., Qing, H., Yuan, D., Zhang, M., Holmden, C., Patterson, W., & Hai, C. (2008). Millennial-scale variability in the asian monsoon: Evidence from oxygen isotope records from stalagmites in southeastern china. *Palaeogeography, Palaeoclimatology, Palaeoecology*, 266(1), 3–12.
- Dansgaard, W. (1964). Stable isotopes in precipitation. *Tellus*, 16(4), 436–468.
- Day, J. A., Fung, I., & Risi, C. (2015). Coupling of South and East Asian monsoon precipitation in July–August. *Journal of Climate*, 28(11), 4330–4356.
- Ding, Y., & Chan, J. C. (2005). The East Asian summer monsoon: An overview. *Meteorology and Atmospheric Physics*, 89(1–4), 117–142.
- Dirmeyer, P. A., & Brubaker, K. L. (2007). Characterization of the global hydrologic cycle from a back-trajectory analysis of atmospheric water vapor. *Journal of Hydrometeorology*, 8(1), 20–37.
- Dyer, E. L., Jones, D. B., Nusbaumer, J., Li, H., Collins, O., Vettoretti, G., & Noone, D. (2017). Congo Basin precipitation: Assessing seasonality, regional interactions, and sources of moisture. *Journal of Geophysical Research: Atmospheres*, 122, 6882–6898. <https://doi.org/10.1002/2016JD026240>
- Dykoski, C. A., Edwards, R. Lawrence, Cheng, H., Yuan, D., Cai, Y., Zhang, M., et al. (2005). A high-resolution, absolute-dated Holocene and deglacial Asian monsoon record from Dongge Cave, China. *Earth and Planetary Science Letters*, 233(1), 71–86.
- Hu, J., Emile-Geay, J., Nusbaumer, J., & Noone, D. (2018). Impact of convective activity on precipitation $\delta^{18}\text{O}$ in isotope-enabled general circulation models. *Journal of Geophysical Research: Atmospheres*, 123, 13–595. <https://doi.org/10.1029/2018JD029187>
- Hu, J., Emile-Geay, J., & Partin, J. (2017). Correlation-based interpretations of paleoclimate data—where statistics meet past climates. *Earth and Planetary Science Letters*, 459, 362–371.
- Hu, C., Henderson, G. M., Huang, J., Xie, S., Sun, Y., & Johnson, K. R. (2008). Quantification of Holocene Asian monsoon rainfall from spatially separated cave records. *Earth and Planetary Science Letters*, 266(3), 221–232.
- Ishizaki, Y., Yoshimura, K., Kanae, S., Kimoto, M., Kurita, N., & Oki, T. (2012). Interannual variability of H_2^{18}O in precipitation over the Asian monsoon region. *Journal of Geophysical Research*, 117, D16308. <https://doi.org/10.1029/2011JD015890>
- Jones, I. C., & Banner, J. L. (2003). Estimating recharge thresholds in tropical karst island aquifers: Barbados, Puerto Rico and Guam. *Journal of Hydrology*, 278(1–4), 131–143.
- Kathayat, G., Cheng, H., Sinha, A., Spötl, C., Edwards, R. L., Zhang, H., et al. (2016). Indian monsoon variability on millennial-orbital timescales. *Scientific reports*, 6, 24374.
- Kong, W., Swenson, L. M., & Chiang, J. C. (2017). Seasonal transitions and the westerly jet in the holocene east asian summer monsoon. *Journal of Climate*, 30(9), 3343–3365.
- Kurita, N., Noone, D., Risi, C., Schmidt, G. A., Yamada, H., & Yoneyama, K. (2011). Intraseasonal isotopic variation associated with the Madden-Julian Oscillation. *Journal of Geophysical Research*, 116, D24101. <https://doi.org/10.1029/2010JD015209>
- Lau, K., Yang, G., & Shen, S. (1988). Seasonal and intraseasonal climatology of summer monsoon rainfall over East Asia. *Monthly Weather Review*, 116(1), 18–37.
- Lee, J.-E., & Fung, I. (2008). “Amount effect” of water isotopes and quantitative analysis of post-condensation processes. *Hydrological Processes*, 22(1), 1–8.
- Li, Y., Wang, N., Zhou, X., Zhang, C., & Wang, Y. (2014). Synchronous or asynchronous Holocene Indian and East Asian summer monsoon evolution: A synthesis on Holocene Asian summer monsoon simulations, records and modern monsoon indices. *Global and Planetary Change*, 116, 30–40.
- Liu, Z., Wen, X., Brady, E., Otto-Bliesner, B., Yu, G., Lu, H., et al. (2014). Chinese cave records and the East Asia summer monsoon. *Quaternary Science Reviews*, 83, 115–128.
- Maher, B. A., & Thompson, R. (2012). Oxygen isotopes from Chinese caves: Records not of monsoon rainfall but of circulation regime. *Journal of Quaternary Science*, 27(6), 615–624.
- McDermott, F. (2004). Palaeo-climate reconstruction from stable isotope variations in speleothems: A review. *Quaternary Science Reviews*, 23(7–8), 901–918.
- Nusbaumer, J., & Noone, D. (2018). Numerical evaluation of the modern and future origins of atmospheric river moisture over the West Coast of the United States. *Journal of Geophysical Research: Atmospheres*, 123, 6423–6442. <https://doi.org/10.1029/2017JD028081>
- Nusbaumer, J., Wong, T. E., Bardeen, C., & Noone, D. (2017). Evaluating hydrological processes in the Community Atmosphere Model Version 5 (CAM5) using stable isotope ratios of water. *Journal of Advances in Modeling Earth Systems*, 9, 949–977. <https://doi.org/10.1002/2016MS000839>
- Partin, J. W., Jenson, J. W., Banner, J. L., Quinn, T. M., Taylor, F. W., Sinclair, D., et al. (2012). Relationship between modern rainfall variability, cave dripwater, and stalagmite geochemistry in Guam, USA. *Geochemistry, Geophysics, Geosystems*, 13, Q03013. <https://doi.org/10.1029/2011GC003930>

- Pausata, F. S., Battisti, D. S., Nisancioglu, K. H., & Bitz, C. M. (2011). Chinese stalagmite $\delta^{18}\text{O}$ controlled by changes in the Indian monsoon during a simulated Heinrich event. *Nature Geoscience*, 4(7), 474–480.
- Risi, C., Bony, S., & Vimeux, F. (2008). Influence of convective processes on the isotopic composition ($\delta^{18}\text{O}$ and δD) of precipitation and water vapor in the tropics: 2. Physical interpretation of the amount effect. *Journal of Geophysical Research: Atmospheres*, 113, D19306. <https://doi.org/10.1029/2008JD009943>
- Roe, G. H., Ding, Q., Battisti, D. S., Molnar, P., Clark, M. K., & Garzione, C. N. (2016). A modeling study of the response of Asian summertime climate to the largest geologic forcings of the past 50 ma. *Journal of Geophysical Research: Atmospheres*, 121, 5453–5470. <https://doi.org/10.1002/2015JD024370>
- Singh, H., Bitz, C., Nusbaumer, J., & Noone, D. (2016). A mathematical framework for analysis of water tracers: Part 1: Development of theory and application to the preindustrial mean state. *Journal of Advances in Modeling Earth Systems*, 8, 991–1013. <https://doi.org/10.1002/2016MS000649>
- Singh, H. K., Donohoe, A., Bitz, C. M., Nusbaumer, J., & Noone, D. C. (2016). Greater aerial moisture transport distances with warming amplify interbasin salinity contrasts. *Geophysical Research Letters*, 43, 8677–8684. <https://doi.org/10.1002/2016GL069796>
- Sinha, A., Berkelhammer, M., Stott, L., Mudelsee, M., Cheng, H., & Biswas, J. (2011). The leading mode of Indian summer monsoon precipitation variability during the last millennium. *Geophysical Research Letters*, 38, L15703. <https://doi.org/10.1029/2011GL047713>
- Sinha, A., Kathayat, G., Cheng, H., Breitenbach, S. F., Berkelhammer, M., Mudelsee, M., et al. (2015). Trends and oscillations in the Indian summer monsoon rainfall over the last two millennia. *Nature Communications*, 6, ncomms7309.
- Stein, A., Draxler, R. R., Rolph, G. D., Stunder, B. J., Cohen, M., & Ngan, F. (2015). NOAA's HYSPLIT atmospheric transport and dispersion modeling system. *Bulletin of the American Meteorological Society*, 96(12), 2059–2077.
- Stohl, A., Cooper, O., & James, P. (2004). A cautionary note on the use of meteorological analysis fields for quantifying atmospheric mixing. *Journal of the Atmospheric Sciences*, 61(12), 1446–1453.
- Tabor, C. R., Otto-Biesner, B. L., Brady, E. C., Nusbaumer, J., Zhu, J., Erb, M. P., et al. (2018). Interpreting precession driven $\delta^{18}\text{O}$ variability in the South Asian monsoon region. *Journal of Geophysical Research: Atmospheres*, 123, 5927–5946. <https://doi.org/10.1029/2018JD028424>
- Tan, M. (2014). Circulation effect: Response of precipitation $\delta^{18}\text{O}$ to the ENSO cycle in monsoon regions of China. *Climate Dynamics*, 42(3–4), 1067–1077.
- Tan, L., Cai, Y., An, Z., Edwards, R. L., Cheng, H., Shen, C.-C., & Zhang, H. (2011). Centennial-to decadal-scale monsoon precipitation variability in the semi-humid region, northern China during the last 1860 years: Records from stalagmites in Huangye Cave. *The Holocene*, 21(2), 287–296.
- Tan, L., Cai, Y., Cheng, H., Edwards, R. L., Shen, C.-C., Gao, Y., & An, Z. (2015). Climate significance of speleothem $\delta^{18}\text{O}$ from central China on decadal timescale. *Journal of Asian Earth Sciences*, 106, 150–155.
- Wan, N.-J., Li, H.-C., Liu, Z.-Q., Yang, H.-Y., Yuan, D.-X., & Chen, Y.-H. (2011). Spatial variations of monsoonal rain in eastern China: Instrumental, historic and speleothem records. *Journal of Asian Earth Sciences*, 40(6), 1139–1150.
- Wang, B. (2002). Rainy season of the Asian-Pacific summer monsoon. *Journal of Climate*, 15(4), 386–398.
- Wang, Y.-J., Cheng, H., Edwards, R. Lawrence, An, Z., Wu, J., Shen, C.-C., & Dorale, J. A. (2001). A high-resolution absolute-dated late Pleistocene monsoon record from Hulu Cave, China. *Science*, 294(5550), 2345–2348.
- Wang, Y., Cheng, H., Edwards, R. L., Kong, X., Shao, X., Chen, S., et al. (2008). Millennial-and orbital-scale changes in the East Asian monsoon over the past 224,000 years. *Nature*, 451(7182), 1090–1093.
- Wang, B., Wu, Z., Li, J., Liu, J., Chang, C.-P., Ding, Y., & Wu, G. (2008). How to measure the strength of the East Asian summer monsoon. *Journal of Climate*, 21(17), 4449–4463.
- Wong, T. E., Nusbaumer, J., & Noone, D. C. (2017). Evaluation of modeled land-atmosphere exchanges with a comprehensive water isotope fractionation scheme in version 4 of the Community Land Model. *Journal of Advances in Modeling Earth Systems*, 9, 978–1001. <https://doi.org/10.1029/2016MS000842>
- Xue, G., Cai, Y., Ma, L., Cheng, X., Cheng, H., Edwards, R. L., et al. (2019). A new speleothem record of the penultimate deglacial: Insights into spatial variability and centennial-scale instabilities of East Asian monsoon. *Quaternary Science Reviews*, 210, 113–124.
- Yang, H., Johnson, K., Griffiths, M., & Yoshimura, K. (2016). Interannual controls on oxygen isotope variability in Asian monsoon precipitation and implications for paleoclimate reconstructions. *Journal of Geophysical Research: Atmospheres*, 121, 8410–8428. <https://doi.org/10.1002/2015JD024683>
- Yoshimura, K., Kanamitsu, M., Noone, D., & Oki, T. (2008). Historical isotope simulation using reanalysis atmospheric data. *Journal of Geophysical Research*, 113, D19108. <https://doi.org/10.1029/2008JD010074>
- Yu, R., & Zhou, T. (2007). Seasonality and three-dimensional structure of interdecadal change in the East Asian monsoon. *Journal of Climate*, 20(21), 5344–5355.
- Yuan, D., Cheng, H., Edwards, R. Lawrence, Dykoski, C. A., Kelly, M. J., Zhang, M., et al. (2004). Timing, duration, and transitions of the last interglacial Asian monsoon. *Science*, 304(5670), 575–578.
- Zhang, H., Ait Brahim, Y., Li, H., Zhao, J., Kathayat, G., Tian, Y., et al. (2019). The Asian summer monsoon: Teleconnections and forcing mechanisms—A review from Chinese speleothem $\delta^{18}\text{O}$ records. *Quaternary*, 2(3), 26.
- Zhang, H., Griffiths, M. L., Chiang, J. C., Kong, W., Wu, S., Atwood, A., et al. (2018). East Asian hydroclimate modulated by the position of the westerlies during Termination I. *Science*, 362(6414), 580–583.
- Zhang, J., Liu, Z., Brady, E. C., Oppo, D. W., Clark, P. U., Jahn, A., et al. (2017). Asynchronous warming and $\delta^{18}\text{O}$ evolution of deep Atlantic water masses during the last deglaciation. *Proceedings of the National Academy of Sciences*, 114(42), 11075–11080.